Self-consistent relativistic calculation of the energy bands and cohesive energy of W

D. M. Bylander and Leonard Kleinman
Department of Physics, University of Texas, Austin, Texas 78712
(Received 6 September 1983)

The energy bands, equilibrium lattice constant, cohesive energy, and bulk modulus of tungsten have been calculated with the use of our relativistic pseudopotential. This is the first self-consistent calculation for W of which we are aware in which the spin-orbit interaction is treated on an equal footing with the other relativistic contributions. The calculated lattice constant and cohesive energy are in good agreement with experiment but the bulk modulus is not.

I. INTRODUCTION

The energy bands of bulk bcc W have been calculated with a nonrelativistic and non-self-consistent muffin-tin Hamiltonian,[1] with fully relativistic but non-self-consistent muffin-tin Hamiltonians,[2] with a self-consistent but nonrelativistic Hamiltonian,[3] and with semirelativistic self-consistent Hamiltonians.[4,5] We here present the first fully relativistic self-consistent calculation of the energy bands, cohesive energy, equilibrium lattice constant, and bulk modulus of W. Our ability to perform this calculation without an inordinate amount of computer time is a consequence of the simplification resulting from the relativistic pseudopotentials which we have recently developed.[6,7] That the Dirac equation can be replaced by a Schrödinger equation containing a simple pseudopotential follows from the fact that relativistic corrections are of importance only in the core region. In Appendix A we review the pseudopotential. The form of the pseudopotential, Eq. (A7), actually used in this calculation was not explicitly written previously due to space limitations in Ref. 7. The $V_l^{\rm ion}(r)$ of Eq. (A3) are displayed in Fig. 2 of Ref. 5 and the $V_l^{\rm so}(r)$ (so is the spin orbit) of Eq. (A2) are displayed here in Fig. 1. The small negative region of $V_d^{\rm so}$ which occurs in a region where the atomic $(r\psi_d)^2$ is $\frac{1}{3}$ or less of its maximum value is nevertheless unfortunate since it undoubtedly makes the so pseudopotentials less transferable from the ion, for which it was calculated and for which it is exact, to the crystal. Other workers[8] have obtained similar sign changes in $V_l^{\rm so}$ which arise from a crossing of the $j=l+\frac{1}{2}$ and $j=l-\frac{1}{2}$ pseudopotential curves.

In Ref. 5 we discussed the convergence of one-electron eigenvalues at high-symmetry points in the Brillouin zone (BZ) by comparing results obtained with our 34-basis-function set (three s, p, and d and one f Gaussians) to an 887-plane-wave basis set. We used the same set here (68 basis functions in this case because of spin) and then to improve the convergence, a mixed basis set consisting of one s and p and two d Gaussians plus all plane waves with $k^2<50(\pi/a)^2$, i.e., at Γ all plane waves through $(2\pi/a)$ (2,2,2). The largest secular determinant obtained throughout the BZ was of size 232×232 with complex entries. The convergence at points Γ and H was improved by about 70%. The binding energy increased by 0.07 eV on going from the former to the latter basis set and, assuming total energies converge at the same rate as one-electron energies, leads us to estimate that the remaining convergence error in the cohesive and binding energies is about 0.03 eV.

II. ENERGY BANDS AND COHESIVE ENERGY

The self-consistent calculation was performed with the same 50-point sample in the $\frac{1}{48}$th irreducible wedge of the BZ and with the same Gaussian weighting used in Ref. 5. In Fig. 2 we display the energy bands calculated for lattice constant $a=5.972$ bohr. After self-consistency was achieved the bands were calculated at all the points indicated by tick marks on the abscissa of the figure. In Table I we compare our eigenvalues with those of Christensen and Feuerbacher[2] (CF). They performed the calculation

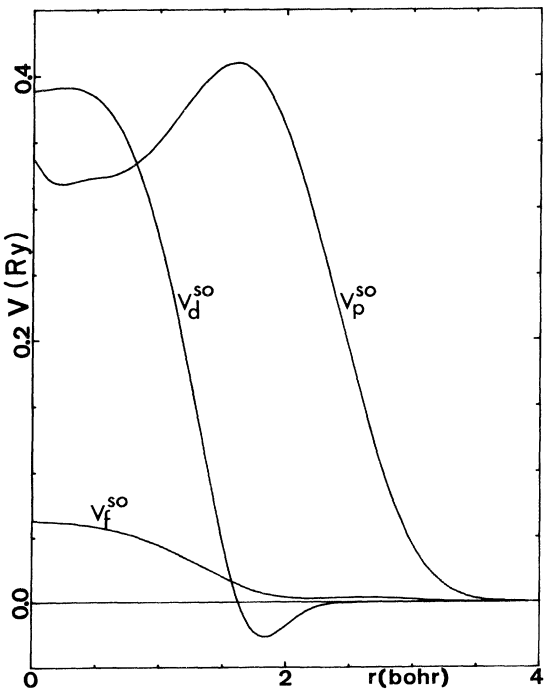

FIG. 1. Spin-orbit pseudopotentials $V_l^{\rm so}$ for W.

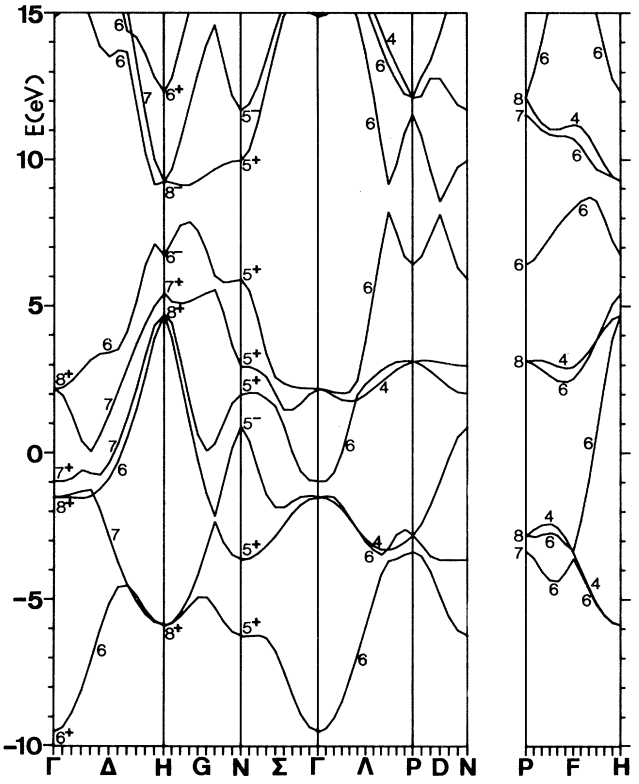

FIG. 2. Relativistic energy bands of W for lattice constant $a = 5.792$ bohr.

for several lattice constants and non-self-consistent potentials. Those in Table I are for $a = 5.981$ bohr (the room-temperature lattice constant) and Slater exchange. Our calculation was performed[5] with relativistic Kohn-Sham exchange[9,10] and Wigner correlation. In Kohn-Sham theory, the one-electron eigenvalues are in principle meaningless. In practice for metals they are a good approximation to the measured excitation energies with the worst errors occurring in the relative positions of bands of different symmetry. Since the Fermi energy is mainly determined by the d bands, one would expect the position of the bottom of the p bands relative to E_F to be a severe test of the energy-band calculation. Although the position of the lowest N_5^- level which is the bottom of the p bands has not been determined experimentally, the dimensions of the hole ellipsoid around it have.[11] In Table II we compare k_F measured in Å^{-1} away from point N in the Σ, D, and G directions with experiment and with calculations of CF (Ref. 2) made at two lattice constants.[12] The Fermi energy used by CF here was not calculated but chosen to give a good fit to other pieces of the Fermi surface. We note that the size of the hole ellipsoid is extremely sensitive to lattice constant and a comparison of the size of our calculated ellipsoid with experiment indicates that our N_5^- lies a few tenths of an eV too high above E_F. Errors of this magnitude in first-principles local-density approximation calculations are not unusual for the relative position

TABLE I. Comparison of our eigenvalues (designated as BK) at high-symmetry points with those of CF (Ref. 2). The asterisk identifies a state whose degeneracy in Ref. 2 appear to be incorrect. The lattice constants used in the two calculations are 5.972 and 5.981 bohr, respectively.

	CF	BK
Γ_6^+	−9.740	−9.521
Γ_8^+	−1.170	−1.531
Γ_7^+	−0.607	−1.007
Γ_8^+	1.986	2.146
Γ_7^-	14.428	14.853
Γ_8^-	14.442*	14.866
Γ_6^+	14.457	16.478
P_7	−3.401	−3.384
P_8	−2.830	−2.822
P_8	3.102	3.099
P_6	6.868	6.407
P_7	11.268	11.527
P_8	11.820	12.104
P_6		18.518
H_8^+	−6.054	−5.902
H_8^+	4.707	4.685
H_7^+	5.401	5.408
H_6^-	6.541	6.703
H_8^-	8.993	9.238
H_6^-	15.518	12.306
N_5^+	−6.256	−6.272
N_5^+	−3.354	−3.663
N_5^-	0.170	0.871
N_5^+	1.959	1.978
N_5^+	2.891	2.938
N_5^+	5.902	5.882
N_5^+	10.711	9.972
N_5^-	11.060	11.672
N_5^-	17.107	16.092
N_5^+		18.066

of states of different symmetry. Feuerbacher and Christensen[13] have determined from photoemission data that the onset of transitions from the third Σ band where it crosses E_F near point N to the seventh Σ band occurs at 10.1 eV. At the experimental point where the Σ band crosses E_F our seventh Σ band lies 10.27 eV above E_F whereas CF's lies about 11 eV above E_F. The major

TABLE II. N_5^- level (in eV above E_F) and the Fermi-surface dimensions in Å^{-1} in three directions compared with two calculations (at lattice constants shown in bohr) from Ref. 2 and with experiment.

	BK (5.972)	CF (5.981)	CF (5.973)	Expt.
N_5^-	0.871	0.170		
$k_F(\Sigma)$	0.217	0.087	0.124	0.143
$k_F(D)$	0.291	0.120	0.173	0.195
$k_F(G)$	0.178	0.075	0.106	0.121

TABLE III. Contributions to the binding energy of tungsten (in rydbergs) for three different lattice constants and the cohesive energy in eV. The last row is the cohesive energy when the calculation was repeated using a tetrahedron integration scheme.

a (bohr)	5.793	5.972	6.151
$\sum_{n,k}\epsilon_n(\vec{k})$	5.986 150	5.345 805	4.769 952
$-\frac{1}{2}8\pi\Omega\sum_{\vec{K}}'\rho^2(\vec{K})/K^2$	−0.090 698	−0.121 795	−0.161 482
$-\int V_{xc}(\rho_T)\rho_{val}$	6.963 418	6.811 623	6.680 444
$\int[\epsilon_{xc}(\rho_T)\rho_T-\epsilon_{xc}(\rho_{core})\rho_{core}]$	−6.224 062	−6.087 135	−5.971 412
E_{Ewald}	−22.615 660	−21.937 796	−21.299 384
$-E_{binding}$	−15.980 852	−15.989 297	−15.981 882
E_{atom}	15.324 816	15.324 816	15.324 816
$E_{cohesive}$ (eV)	8.9254	9.0403	8.9394
Tetrahedron (eV)	8.8494	8.9775	8.8863

discrepancy between CF and us in Table I is in the high-lying Γ levels, and this appears to be due to a misprint in their Table II. They list three twofold degenerate levels which are nearly degenerate but mention in the text a twofold and a fourfold level which are nearly degenerate, which is what we find.

We note the so-called energy dependence[4] of the spin-orbit interaction. The splitting of the $\Gamma_{25'}$ and $H_{25'}$ d states into Γ_8^+ and Γ_7^+ at −1.531 and −1.007 eV and H_8^+ and H_7^+ at 4.685 and 5.408 eV is larger at point H because the phase introduced by the finite wave vector turns states which are bonding at point Γ into antibonding states at point H. Antibonding wave functions, since they vanish between atoms, must have larger amplitudes than bonding functions in the core region and therefore have larger spin-orbit splittings. The H_{15} p state splits into H_6^- and H_8^- with a splitting more than four times larger than the P_4 state which splits into P_7 and P_8 at 11.527 and 12.104 eV. This is due in part to the fact that P_4 is mixed p and f symmetry whereas H_{15} is almost of pure p character. Finally we note that the Γ_{25} state (which contains no spherical harmonics below f) lying 29.9 eV above the bottom of the valence bands in Ref. 5 is barely split into Γ_7^- and Γ_8^- levels here lying only 24.38 eV above the bottom of the bands. This is due to the far better convergence achieved here with 87 plane waves than obtained previously with a single f Gaussian.

Table III lists the various contributions to the binding and cohesive energy for three lattice constants. The first entry, the sum of the one-electron energies of occupied states, contains the spin-orbit[14] as well as other contributions to the binding energy. A discussion is given in Ref. 5 concerning how the otherwise arbitrary zero of Coulomb potential is included in the one-electron energies so as to be consistent with the Ewald contribution to the binding energy. The second entry subtracts half the valence Coulomb self-interaction which is counted twice in summing the one-electron energies. The third entry subtracts the exchange-correlation contribution to the one-electron energies and the fourth entry adds the exchange-correlation contribution to the binding energy. As in Ref. 5, because of the nonlinearity of the exchange and correlation potentials and energy functionals, the valence terms are not separable from the core and we work with the total charge density ρ_T. [The ionic pseudopotential is formed by subtracting $V_{xc}^{val}=V_{xc}(\rho_T)-V_{xc}(\rho_{core})$ as well as the valence Coulomb potential from the atomic pseudopotential.] ρ_{core} is taken to be rigid so the $V_{xc}(\rho_{core})$ term is cancelled when the self-consistent V_{xc}^{val} is added to the ionic pseudopotential. Similarly the ρ_{core} term in the exchange energy (fourth entry of Table III) also occurs in the atomic valence total energy but does not cancel in the cohesive energy[15] because of core-core overlap in the crystal. The cohesive energy obtained by adding $-E_{binding}$ to E_{atom} is given in the next to last row of Table III. Fitting $E_{cohesive}$ at the three values of lattice constant with a parabola, the equilibrium lattice constant, cohesive energy, and bulk modulus are obtained and compared with experiment in Table IV. We[16] have recently calculated the total valence electron energy of W and Mo atoms in d^5s and d^4s^2 configurations with broken symmetry so that the single Slater determinant required by the local-spin-density approximation could account for both the exchange energy which forces the spins to be nearly parallel

TABLE IV. Comparison with experiment of lattice constant (at 4.2 K), cohesive energy, and bulk modulus of tungsten calculated with two $\vec{k}$-space integration schemes and also with the inclusion of core overlap contributions to the exchange-correlation energy (with tetrahedron integration).

	Gaussian	Tetrahedron	Core	Expt.
a (Å)	3.163	3.168	3.155	3.162
$E_{cohesive}$ (eV)	9.0404	8.9783	9.0638	8.90
B (10^{12} erg/cm^3)	2.703	2.747	2.609	3.232

and the spin-orbit energy which mixes the spin directions. For Mo, where the sixfold ionization energy is known, an error of 0.43 Ry was obtained and a similar error is presumed for W. These are due almost entirely to the local-density approximation and also occur in the crystal; this accounts for the good agreement between theory and experiment in the cohesive energy. The atomic energy in Table III is for the calculated d^5s ground state even though experimentally the d^4s^2 configuration is the ground state, lying 0.366 eV below the d^5s. Thus one might expect the calculated cohesive energy to be a little too large, as it is, due to the fact that the atomic valence binding energy which was subtracted from the crystal binding energy was not that of the ground state. We note in passing that our nominally $^7S_3$ d^5s calculated atomic ground-state energy contained 0.174 eV of spin-orbit energy without which it would not have been the ground state. This would be obtained in ordinary calculations by admixing $^5P_3$ terms with the $^7S_3$. We also note that the cancellation of local-density-approximation errors is best when the atom and crystal are in approximately the same configuration. Since the projected[17] configuration of the crystal is $f^{0.075}d^{4.828}p^{0.842}s^{0.254}$, it would not be correct to calculate the cohesive energy with an atomic energy taken to be the d^5s energy plus the 0.366 eV that the true ground state lies below it. Our calculated lattice constant is seen to be in excellent agreement with the 4.2-K lattice constant and our bulk modulus in only fair agreement with experiment.

Although our 50-point Gaussian weighted[5] sampling of the $\frac{1}{48}$th wedge of the BZ would appear adequate when compared with the 14-point sampling used elsewhere,[3] we decided to repeat the entire self-consistent calculation using the same 50 $\vec{k}$ points but evaluating all BZ sums with the tetrahedron integration scheme.[18,19] We recently pointed out[20] that this scheme has heretofore been incorrectly applied and showed how to use it with some lattices. In Appendix B we describe how the tetrahedra are constructed for our particular case of a bcc lattice of points in a bcc BZ (i.e., fcc reciprocal space). We show only the cohesive energy obtained in the last row of Table III for three lattice constants and the equilibrium lattice constant, cohesive energy, and bulk modulus in Table IV. The improvement over the Gaussian sampling for the cohesive energy may be fortuitous when our discussion of the atomic energy is considered, the improvement in the bulk modulus is almost negligible and the equilibrium lattice constant, though still within acceptable agreement with experiment, is poor when compared with the Gaussian sampling result. In the third column in Table IV we list the results that are obtained if ρ_{core} for a single atom is substituted for the superposed atomic core charges in $-\epsilon_{\text{xc}}(\rho_{\text{core}})\rho_{\text{core}}$ which appears in the fourth contribution to E_{binding} in Table III. This adds the longest-range core-core interaction to the binding energy. It is what passes for the van der Waals interaction in the local-density approximation. Since it is attractive and increases rapidly with decreasing lattice constant, it increases the cohesive energy and decreases the equilibrium lattice constant and bulk modulus. Thus we see that to within uncertainties arising from core-core interactions and configurational differences between the crystal and the atom, the relativistic pseudopotential used in conjunction with the local-spin-density approximation yields the cohesive energy and equilibrium lattice constant highly accurately but yields a bulk modulus about 15% too small. This perhaps is due to the lack of perfect transferability of the pseudopotential. The pseudopotential which is exact for a W^+ ion in a particular configuration gave errors of about 6 meV in one-electron eigenvalues of a W atom.[5] A relative error of 36 meV (there are six valence electrons per atom) between the cohesive energies calculated at two lattice constants is more than enough to account for the error in the bulk modulus.

ACKNOWLEDGMENTS

This work was supported by the Robert A. Welch Foundation by the National Science Foundation under Grant No. DMR-80-19518.

APPENDIX A

In Ref. 6 we obtained an ionic pseudopotential,

$$V_{Ps}^{\text{ion}}(r)=\sum_{j=l-1/2}^{l+1/2}\sum_{l,m}|\Phi_{jlm}(\theta,\phi)\rangle V_{jl}^{\text{ion}}(r)\langle\Phi_{jlm}(\theta,\phi)|$$
$$=\sum_{j=l-1/2}^{l+1/2}\sum_{l,m}|\Phi_{jlm}(\theta,\phi)\rangle[V_l^{\text{so}}(r)\vec{\mathbf{L}}\cdot\vec{\mathbf{S}}+\bar{V}_l^{\text{ion}}(r)]\langle\Phi_{jlm}(\theta,\phi)|$$
$$=\sum_{l,m,\sigma}|\chi_\sigma Y_{lm}(\theta,\phi)\rangle[V_l^{\text{so}}(r)\vec{\mathbf{L}}\cdot\vec{\mathbf{S}}+\bar{V}_l^{\text{ion}}(r)]\langle Y_{lm}(\theta,\phi)\chi_\sigma|\ , \tag{A1}$$

which when used in the Schrödinger equation contained all relativistic contributions to order α^2 (not $Z^2\alpha^2$) where α is the fine-structure constant. Here

$$V_l^{\text{so}}=\frac{2}{2l+1}(V_{j=l+1/2}^{\text{ion}}-V_{j=l-1/2}^{\text{ion}})\ , \tag{A2}$$

$$\bar{V}_l^{\text{ion}}=\frac{1}{2l+1}[(l+1)V_{j=l+1/2}^{\text{ion}}+lV_{j=l-1/2}^{\text{ion}}]\ , \tag{A3}$$

Y_{lm} is a spherical harmonic, χ_σ is a spin-$\frac{1}{2}$ function, and Φ_{jlm} is an eigenfunction of total angular momentum j. That the second line of Eq. (A1) is equivalent to the first line is easily seen by observing that all matrix elements are identical for the two. The third line results from changing from an $(lsjm)$ representation to an $(lms\sigma)$.

Note that because $V_{Ps}^{\rm ion}(r)$ is semilocal (i.e., nonlocal in θ and ϕ but local in r), when crystal wave functions are expanded in localized orbitals, matrix elements of $V_{Ps}^{\rm ion}(r)$ consist of $n^2/2$ different three-center integrals of the form

$$\int V(r)\delta(r-r')f_1(\vec{r}-\vec{R}_1)f_2(\vec{r}'-\vec{R}_2)Y_{lm}(\theta,\phi)Y_{lm}(\theta',\phi')d^3r\,d^3r' ,$$

where n is the number of localized orbitals $f_i(\vec{r}-\vec{R}_j)$ which overlap the pseudopotential located at the origin. To obtain a completely nonlocal pseudopotential which leads to matrix elements consisting of products of two-center integrals, of which there are only n, we[7] first define $\delta V_{jl}(r)=V_{jl}(r)-V_L(r)$, where $V_L(r)$ is an arbitrary average local pseudopotential so that

$$V_{Ps}^{\rm ion}(r)=V_L^{\rm ion}(r)+V_{\rm SL}^{\rm ion}(r) , \tag{A4}$$

where (SL is the semilocal and NL is the nonlocal pseudopotential)

$$V_{\rm SL}^{\rm ion}(r)=\sum_{j,l,m} |\,\Phi_{jlm}(\theta,\phi)\rangle\delta V_{jl}^{\rm ion}(r)\langle\Phi_{jlm}(\theta,\phi)\,| \ . \tag{A5}$$

We then construct a nonlocal pseudopotential to replace $V_{\rm SL}$,

$$V_{\rm NL}^{\rm ion}(r)=\sum_{j,l,m}\frac{|\,F_{jl}(r)\Phi_{jlm}(\theta,\phi)\delta V_{jl}^{\rm ion}(r)\rangle\langle\delta V_{jl}^{\rm ion}(r)\Phi_{jlm}(\theta,\phi)F_{jl}(r)\,|}{\langle F_{jl}(r)\,|\,\delta V_{jl}^{\rm ion}(r)\,|\,F_{jl}(r)\rangle} , \tag{A6}$$

where $F_{jl}(r)$ is the radial eigenfunction of the atomic state from which the pseudopotential was originally obtained. Note that if either $V_{\rm SL}^{\rm ion}$ or $V_{\rm NL}^{\rm ion}$ operates on $|\,F_{jl}(r)\Phi(\theta,\phi)\rangle$ one obtains $|\,F_{jl}(r)\Phi(\theta,\phi)\delta V_{jl}^{\rm ion}(r)\rangle$. However, if the pseudopotential is transported to a different chemical situation so that the eigenfunction on which it operates is not $|\,F_{jl}(r)\Phi(\theta,\phi)\rangle$, $V_{\rm NL}$ yields a slightly different result than $V_{\rm SL}$. The pseudopotential is always only approximate when transported to a different chemical environment so that by a judicious choice of $V_L^{\rm ion}(r)$ and therefore the $\delta V_{jl}^{\rm ion}(r)$, $V_{\rm NL}^{\rm ion}$ can be made to yield more accurate results than $V_{\rm SL}^{\rm ion}$. We have obtained[7] a W^+ pseudopotential and applied both forms to self-consistent calculations of W^{2+} and W. The $6s_{1/2}$, $6p_{1/2}$, $6p_{3/2}$, $5d_{3/2}$, and $5d_{5/2}$, eigenvalues obtained from $V_{\rm NL}^{\rm ion}$ were in every case closer to the eigenvalue obtained from the Dirac equation than was the $V_{\rm SL}^{\rm ion}$ eigenvalue. The pseudopotential used here and in Ref. 5 differs from that of Ref. 7 in that, for reasons discussed in Ref. 5, we used a different form of valence exchange-correlation potential. This resulted in a pseudopotential which is overall more transferable but for which $V_{\rm NL}$ was more transferable than $V_{\rm SL}^{\rm ion}(r)$ only for d electrons. $V_{\rm NL}^{\rm ion}(r)$ is put in a more useful form by letting

$$\Delta V_{jl}^{\rm ion}(r)=F_{lj}(r)\delta V_{jl}^{\rm ion}(r)[\langle F_{jl}(r)\,|\,\delta V_{jl}^{\rm ion}(r)\,|\,F_{jl}(r)\rangle]^{-1/2} .$$

Then

$$\begin{aligned}V_{\rm NL}^{\rm ion}(r)&=\sum_{j,l,m}|\,\Delta V_{jl}^{\rm ion}(r)\Phi_{jlm}(\theta,\phi)\rangle\langle\Phi_{jlm}(\theta,\phi)\Delta V_{jl}^{\rm ion}(r)\,|\\&=\sum_{j,l,m}|\,[\Delta\bar{V}_l^{\rm ion}(r)+\vec{L}\cdot\vec{S}\,\Delta V_l^{\rm so}(r)]\Phi_{jlm}(\theta,\phi)\rangle\langle\Phi_{jlm}(\theta,\phi)[\Delta\bar{V}_l^{\rm ion}(r)+\vec{L}\cdot\vec{S}\,\Delta V_l^{\rm so}(r)]\,|\\&=\sum_{l,m,\sigma}|\,[\Delta\bar{V}_l^{\rm ion}(r)+\vec{L}\cdot\vec{S}\,\Delta V_l^{\rm so}(r)]Y_{lm}(\theta,\phi)\chi_\sigma\rangle\langle\chi_\sigma Y_{lm}(\theta,\phi)[\Delta\bar{V}_l^{\rm ion}(r)+\vec{L}\cdot\vec{S}\,\Delta V_l^{\rm so}(r)]\,| \ .\end{aligned} \tag{A7}$$

Matrix elements of $V_{\rm NL}^{\rm ion}(r)$ are obviously products of two-center integrals.

The nonlocal semirelativistic psuedopotential of Ref. 5 was not obtained by setting $\Delta V_l^{\rm so}=0$ in Eq. (A7) but by setting $V_l^{\rm so}=0$ in Eq. (A1) and calculating a radial atomic eigenfunction of $V_l^{\rm ion}$ which was used to create the nonlocal form of the semirelativistic pseudopotential, i.e., rather than averaging nonlocal $j=l\pm\frac{1}{2}$ pseudopotentials we averaged semilocal $j=l\pm\frac{1}{2}$ pseudopotentials and then made the averaged pseudopotential nonlocal. The two different ways of averaging lead to atomic eigenvalues which differ by less than 1 meV.

APPENDIX B

We have recently pointed out[20] that the tetrahedron integration scheme[18,19] as it has previously been applied in practice seriously misweights the contribution of the various mesh points in the BZ at which the integrand is calculated. We showed how this misweighting (which is due to assuming cubic symmetry when the tetrahedra are oriented so as to destroy it) could be avoided when the tungsten fcc reciprocal space was sampled with a simple cubic mesh or with an fcc mesh. When these calculations were begun (for semirelativistic W) we had not even considered using the tetrahedron scheme and were unaware of the

difficulties associated with it. Thus any cubic array of points with sufficient density in reciprocal space was as good as any other and we happened to choose the bcc mesh $(2\pi/12a)$ (i,j,k) (where i, j, and k are all even or all odd) to sample our fcc reciprocal space.

To perform the tetrahedron integration correctly in this case we expand our integration to the super BZ cube in reciprocal space $-2\pi/a \leq \chi,\eta,\xi \leq 2\pi/a$ which contains the first four bcc BZ. Our mesh consists of body-centered cubes, each of which may be filled with six pyramids whose base is a cube face and whose vertex is the cube center. Each pyramid may be cut into two tetrahedra by a plane containing a base diagonal and the vertex. We thus fill each cube with 12 tetrahedra. We actually do this twice, using both base diagonals to slice each pyramid. This makes all the corners of the body-centered mesh cubes equivalent and thus allows us to reflect all octants of the super BZ into the first octant. Because each tetrahedron has the same volume, the weighting of every point is proportional to the number of tetrahedra touching it (assuming the Fermi surface does not cut through any of the tetrahedra). The cube-center points touch all 24 tetrahedra which doubly fill the cube. For each of the three faces with which they are associated each cube corner touches three tetrahedra (two when the plane slicing the pyramid contains the point and one when it does not), but each mesh cube corner is associated with eight different mesh cubes and thus touches 72 tetrahedra. (Mesh cube corners on the face of the super BZ are also associated with eight mesh cubes when one remembers that points on opposite faces of the super BZ are considered to be the same point.) This 3-to-1 misweighting of cube corners with respect to cube centers is removed by displacing the super BZ by $(2\pi a/12)$ (1,1,1) which interchanges mesh cube corners with mesh cube centers, repeating the integration, and averaging with the previous integration. This slightly complicates the reflection symmetry; all octants are reflected into the "enlarged octant," $-2\pi/12a \leq \chi,\eta,\xi \leq 2\pi \times 13/12a$ with the mesh cubes weighted 1, 2, 4, and 8 according to whether they are corner, edge, face, or interior mesh cubes of the enlarged octant.

[1]I. Petroff and C. R. Viswanathan, Phys. Rev. B 4, 799 (1971).
[2]N. E. Christensen and B. Feuerbacher, Phys. Rev. B 10, 2349 (1974).
[3]A. Zunger and M. L. Cohen, Phys. Rev. B 20, 4082 (1979); 19, 568 (1979).
[4]L. F. Mattheiss and D. R. Hamann (unpublished).
[5]D. M. Bylander and L. Kleinman, Phys. Rev. B 27, 3152 (1983).
[6]L. Kleinman, Phys. Rev. B 21, 2630 (1980).
[7]L. Kleinman and D. M. Bylander, Phys. Rev. Lett. 48, 1452 (1982).
[8]G. B. Bachelet, D. R. Hamann, and M. Schlüter, Phys. Rev. B 26, 4199 (1982).
[9]A. K. Rajagopal, J. Phys. C 11, L943 (1978).
[10]A. K. MacDonald and S. H. Vosko, J. Phys. C 12, 2977 (1979).
[11]V. V. Boiko and V. A. Gasparov, Zh. Eksp. Teor. Fiz. 61, 2362 (1972) [Sov. Phys.—JETP 34, 1266 (1972)].
[12]These are room temperature and an estimate of the 4.2-K lattice constant based on old thermal-expansion data. Based on the data in the third edition of the AIP Handbook we estimate $a_{4.2\,K} = 5.976$ bohr.
[13]B. Feuerbacher and N. E. Christensen, Phys. Rev. B 10, 2373 (1974).
[14]O. Gunnarsson and B. I. Lundqvist, Phys. Rev. B 13, 4274 (1976).
[15]The claim that they do cancel made in Ref. 5 is not correct.
[16]D. M. Bylander and L. Kleinman, Phys. Rev. Lett. 51, 889 (1983).
[17]This comes from a projection onto symmetrically orthogonalized basis functions made in Ref. 5. Because the basis set used here contains plane waves, it would not be very meaningful to make that kind of projection here.
[18]G. Lehman and M. Taut, Phys. Status Solidi B 54, 469 (1971).
[19]D. Jepsen and O. K. Anderson, Solid State Commun. 9, 1763 (1971).
[20]L. Kleinman, Phys. Rev. B 28, 1139 (1983).